Journal of Microelectronics and Electronic Packaging (2010) **7**, 48-57
Copyright © International Microelectronics And Packaging Society
ISSN: 1551-4897

Interfacial Reactions Between Electrodeposited Sn-Cu, Sn-Ag-Cu Solders and Cu, Ni Substrates

Chunfen Han, Qi Liu, and Douglas G. Ivey*

***Abstract*—Interfacial reactions between two near eutectic Pb-free solders, Sn-1.1Cu and Sn-3.6Ag-1.8Cu, and two common base materials, Cu and Ni, were studied by characterizing the formation and growth of intermetallic compounds (IMCs) during reflowing and aging using SEM, XRD, and TEM. A continuous bilayer of thin, uniform Cu_3Sn and thick, nonuniform Cu_6Sn_5 was formed at the interfaces of both Sn-1.1Cu/Cu and Sn-3.6Ag-1.8Cu/Cu, with the Cu_3Sn layer adjacent to the Cu substrate. This is attributed to the diffusion of Cu from the Cu substrate to the solder to first form Cu_6Sn_5, then Cu_3Sn. The inclusion of Ag in the Sn-3.6Ag-1.8Cu solder film inhibited the diffusion of Cu and, therefore, the growth of Cu_3Sn. For both Sn-1.1Cu/Ni and Sn-3.6Ag-1.8Cu/Ni, an intermetallic film of $(Ni,Cu)_3Sn_4$ was formed at the interface, and the film had three distinct morphologies: a continuous planar layer at the Ni interface, followed by long, thin needles and large, polygonal crystals. The layers and the crystals were thinner at the Sn-3.6Ag-1.8Cu/Ni interface, indicating that the addition of Ag slowed down the growth of the $(Ni,Cu)_3Sn_4$ films. At the Sn-3.6Ag-1.8Cu/Ni interface, Ag_3Sn particles were also observed and they coarsened with aging time. No separate Ag particles were observed.**

***Keywords*—Lead-free solder, Sn-Cu, Sn-Ag-Cu, interfacial reactions, diffusion, microstructural characterization**

Introduction

Solders are important joining materials in electronic packages and assemblies [1]. During the past 60 y, eutectic and near-eutectic Pb-Sn solders have been used as the principal joining materials because of their low cost, low melting point (183°C), outstanding solderability, and good mechanical properties [2,3]. Pb-Sn solders are also highly compatible with electronics assembly processes and materials and can form stable joints that are usable under a wide variety of service environments [2,3]. However, increasing health and environmental concerns worldwide regarding the toxicity of Pb have prompted countries such as Japan and those from the European Union to pass legislation prohibiting or restricting the use of Pb-Sn solders [4]. These restrictions have stimulated the development of a large number of Pb-free alternative solders [2,4,5], most of which are Sn-based.

Among available Pb-free solders, eutectic Sn-Cu solder is relatively cheap and is mainly used in wave soldering. In addition, eutectic and near-eutectic Sn-Ag-Cu solder is considered as a prime candidate to replace Pb-Sn solder because of its relatively low melting temperature, good mechanical properties, and relatively good wetting properties [6-8]. Sn-Ag-Cu solder has been used in both reflow and wave soldering [9].

During soldering, interdiffusion and reactions between the molten solder and conductor metals occur. The substrate metal dissolves into the molten solder and simultaneously the active constituents in the solder combine with the substrate metal to form IMCs at the solder/substrate interface [9]. The formation of a thin, continuous, and uniform IMC layer is necessary for good bonding [4,10]. However, due to their inherent brittle nature and tendency to generate structural defects, IMC layers that are too thick (caused by excessive interfacial reactions during soldering or in use) are sensitive to stress and sometimes provide sites for the initiation and propagation of cracks [11,12]. This may lead to poor joint strength and degrade the long term reliability of solder joints [9,12,13]. Moreover, the IMC layer will become thicker during thermal aging due to solid state diffusion [14]. Therefore, it is important to study the formation and growth of IMC layers during high temperature reflow and subsequent aging.

Many studies have been performed on the interfacial reaction and growth mechanism of IMCs between Pb-free solders and Cu and/or Ni substrates during reflow and/or aging. In the Sn-Cu system, Cu_3Sn and Cu_6Sn_5 are the two IMCs formed at the solder/Cu interface. For the Sn-Ni system, three intermetallic phases, Ni_3Sn, Ni_3Sn_2, and Ni_3Sn_4, are stable at temperatures below 300°C, but only the Ni_3Sn_4 phase is frequently found in the solder/Ni couples [15-17]. When a small amount of Cu is added to a Sn-rich solder to form a Cu-bearing solder, such as Sn-Cu and Sn-Ag-Cu solders, ternary IMCs consisting of Sn, Cu, and Ni form after reacting with Ni substrate. It has also been found that as Cu concentration in the solder is increased, the IMCs that form at the solder/Ni interface change from $(Ni,Cu)_3Sn_4$ to $(Cu,Ni)_6Sn_5$ [18-21].

In the Sn-Ag system, only orthorhombic Ag_3Sn exists as an IMC. Large Ag_3Sn intermetallic plates (>30 μm in length) have been reported to form at the Sn-Ag-Cu solder/Cu substrate interface [5,10,22]. These are believed to be detrimental to the mechanical properties of the solder joints by inducing brittle fracture or providing crack initiation sites [8,10,23]. Higher populations of large Ag_3Sn plates are found in Sn-Ag-Cu solders with higher Ag content [10,22].

The objective of this work is to investigate interfacial reactions between Pb-free, Sn-based solders (Sn-1.1Cu and

Manuscript received January 2010 and accepted June 2010
Department of Chemical and Materials Engineering, University of Alberta, Edmonton, Alberta, Canada T6G 2V4
*Corresponding author; e-mail: doug.ivey@ualberta.ca

Downloaded from http://meridian.allenpress.com/jmep/article-pdf/7/1/48/2247362/1551-4897-7_1_48.pdf by guest on 01 November 2022

1551-4897 © 2010 International Microelectronics And Packaging Society

Sn-3.6Ag-1.8Cu solder films) and substrates (Cu and Ni) during reflow and aging. In most previous interfacial reaction studies, commercial solder pastes and solder balls or pure metals assembled with specific compositions were used. In this study, near-eutectic Sn-1.1Cu solder films are electrodeposited from Sn-Cu-citrate solutions and near-eutectic Sn-3.6Ag-1.8Cu solder films are electrodeposited from Sn-Cu-citrate suspensions with Ag nano-particles. For Pb-free solders, reflow processing requires temperatures at least 30°C higher than the melting point [24]. The eutectic temperatures for Sn-Cu and Sn-Ag-Cu are in the 221-227°C range, so that 260°C was chosen as the reflow temperature. Compared with Pb-Sn solder, the higher reflow temperature plus the higher Sn content for both the Sn-Cu and Sn-Ag-Cu solders increase the potential for IMC growth and substrate dissolution at the solder/substrates interface [24]. Microstructural characterization is carried out for Sn-Cu and Sn-Ag-Cu solder films on both Cu and Ni substrates after reflowing and aging for different lengths of time to better understand the formation and growth of IMC layers in the Sn-Cu/Cu, Sn-Cu/Ni, Sn-Ag-Cu/Cu, and Sn-Ag-Cu/Ni systems.

Experimental Methods

The Sn-Cu-citrate solutions were prepared by dissolving triammonium citrate ($(NH_4)_3C_6H_5O_7$, Alfa Aesar, 98%) in deionized water to a concentration of 0.30 mol/L and then dissolving $SnCl_2{\cdot}2H_2O$ (Fisher Scientific) and $CuCl_2{\cdot}2H_2O$ (Fisher Scientific) in the citrate solution to concentrations of 0.22 mol/L and 0.003 mol/L, respectively [25]. Silver particles (Sigma-Aldrich, 100 nm in size) were added to the above Sn-Cu-citrate solution to a concentration of 0.8 g/L after the solution was stabilized for about 1 h [26]. Ultrasonic dispersion and overhead mechanical agitation were used to help disperse the Ag particles.

Silicon wafer pieces, metallized with a 25 nm TiW adhesion layer and a 200 nm Au seed layer, were used as substrates/seed layers for Cu or Ni electrodeposition. Nickel layers (~6 µm thick) electroplated from a standard Watts Ni plating solution onto the Au seed layer were utilized for deposition on Ni. For the Cu samples, Cu layers (~6 µm thick) were electrodeposited from a Cu-citrate solution (containing 0.30 mol/L triammonium citrate and 0.22 mol/L $CuCl_2{\cdot}2H_2O$) onto Au metallized Si wafer pieces. Silicon wafer pieces, metallized with a 25 nm TiW adhesion layer and a 200 nm Pt seed layer, were used as anodes.

A Dynatronix DuPR 10-0.1-0.3 pulse plating power supply was used to pulse current (PC) plate the Sn-Cu and Sn-Ag-Cu solders and the Cu substrate layer, with a 2 ms forward on-time and 8 ms forward off-time, and to DC plate the Ni substrate layer. All the Sn-Cu solder films were plated at a current density of 10 mA/cm^2 for 20 min without agitation and Sn-Ag-Cu solder films were plated at a current density of 40 mA/cm^2 for 8 min with a stirring speed of 600 rpm. Copper was plated at a current density of 10 mA/cm^2 for 30 min without agitation. All electrodeposition of Sn-Cu, Sn-Ag-Cu, and Cu was done at room temperature. Nickel was plated at a current density of 50 mA/cm^2 for 10 min. The temperature was kept at 50°C and the stirring speed was set at 80 rpm using a magnetic stirrer and hot plate.

An RC2400 Bio-Rad alloying furnace was used to reflow and age Sn-Cu and Sn-Ag-Cu samples. The reflow process was done in a forming gas (95 vol% N_2 + 5 vol% H_2) atmosphere with a heating rate of 400°C/min and a cooling rate of 100°C/min. The as-deposited samples were reflowed at 260°C for 30-90 s. The aging treatment was carried out for reflowed samples by keeping the temperature at 125°C, which is a typical aging temperature used in the literature [23,27,28], for 24, 48, and 72 h in the same forming gas atmosphere.

The microstructure and composition of both the Sn-Cu and Sn-Ag-Cu films were characterized using a Hitachi H2700 scanning electron microscope (SEM) equipped with an ultra-thin window energy dispersive x-ray (EDX) spectrometer. Deposit compositions were found by averaging measurements taken from at least three regions, each 400 × 400 µm^2 in size. Analysis was done at 20 kV with a working distance of 17 mm and a count rate of 2500-4000 counts/s. Cross section samples were prepared by cleaving (Si substrates) using a diamond pen. After sectioning, the samples were mounted with epoxy resin, then ground with SiC papers (240, 320, 400, 600, 1200, and 4000 grit) in sequence and finally polished with a 0.05 µm diameter Al_2O_3 particle suspension.

Phase analysis was performed using thin film x-ray diffraction (XRD) with a Rigaku rotating Co anode system, operating in continuous scanning mode at a voltage of 40 kV and a current of 160 mA. The samples were scanned from 20° to 100° at a rate of 3°/min.

Transmission electron microscopy, using a JEOL 2010 TEM operated at 200 kV, was used to conclusively identify the IMCs. Two different methods were used to prepare TEM samples. Cross section samples were prepared by mechanical dimpling followed by sputtering. An extraction method was also used to prepare TEM samples of isolated IMCs.

Results and Discussion

A. Sn-Cu Solder

1. Sn-Cu Solder and Cu Substrates

Near eutectic Sn-Cu (1.1 wt% Cu) solder films were electrodeposited onto Cu layers. After reflow at 260°C for 90 s, the entire sample surface was covered with melted solder that had resolidified. Fig. 1(a) (low magnification) and Fig. 1(b) (high magnification) show SEM backscattered electron (BSE) cross section images of Sn-Cu/Cu after

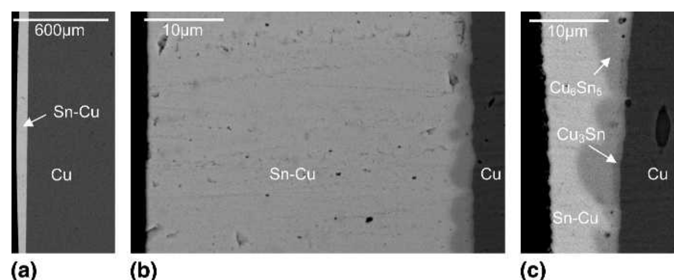

Fig. 1. SEM BSE cross section images of Sn-Cu films electrodeposited onto Cu after reflow at 260°C for 90 s. (a) Sn-Cu/Cu interface at low magnification; (b) Sn-Cu/Cu interface at higher magnification; (c) Sn-Cu/Cu interface after etching away most of the solder layer.

Downloaded from http://meridian.allenpress.com/jmep/article-pdf/7/1/48/2247362/1551-4897-7_1_48.pdf by guest on 01 November 2022

reflow and resolidification. The low contact angle shown in Fig. 1(a) indicates that the Sn-Cu solder has good wettability to the Cu substrate. At high magnification [Fig. 1(b)], a reacted region was observed at the Cu/Sn-Cu interface. In order to further study the interfacial layers, a solution (2% HCl + 5%HNO_3 + 93%CH_3OH) was used to selectively etch most of the Sn matrix away, and the corresponding SEM BSE cross section image of the reflowed Sn-Cu/Cu sample is shown in Fig. 1(c). There are two continuous layers of IMCs formed between the Cu substrate and the Sn-Cu solder. One layer is thin and is adjacent to the Cu substrate; it possesses a darker color and has a composition of ~62 wt% Cu (~75 at% Cu) which is close to the composition for Cu_3Sn. The other layer is thicker and situated between the Cu_3Sn layer and the Sn-Cu solder. It is characterized by a brighter color and has a composition of ~40 wt% Cu (~55 at% Cu), which is close to the composition for Cu_6Sn_5.

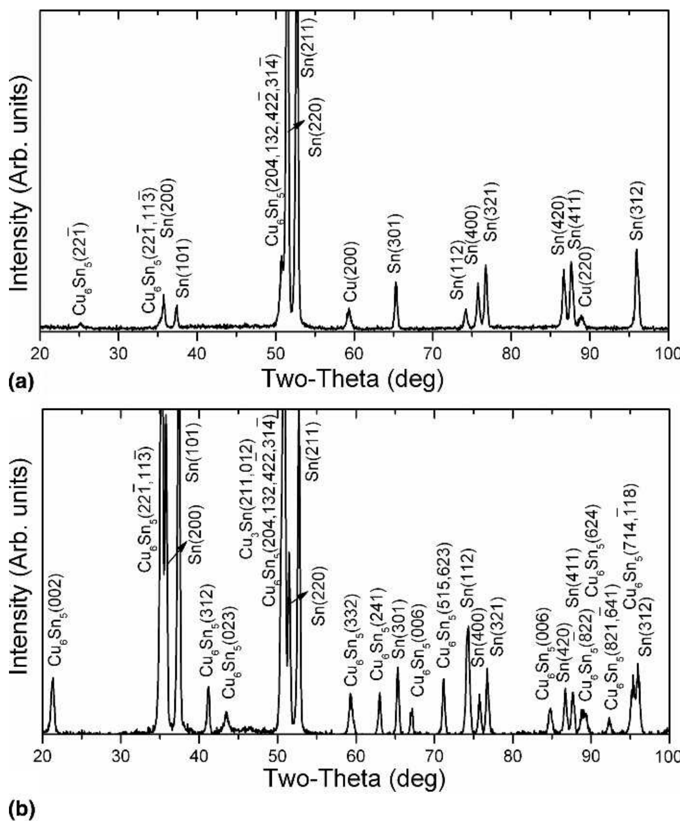

Fig. 2. XRD patterns of Sn-Cu solder films electrodeposited onto Cu. (a) As-deposited sample; (b) after reflow at 260°C for 90 s.

XRD analysis was carried out to verify the identity of the phases in the Sn-Cu/Cu system before and after reflow and the results are shown in Fig. 2. Before reflow [Fig. 2(a)], three different phases were detected. Copper peaks at 59.3° and 88.9° are from the Cu substrate. The main phase in the Sn-Cu deposit is Sn with a small amount of Cu_6Sn_5. After reflow (Fig. 2b), the Cu_6Sn_5 peaks increased in intensity and additional Cu_6Sn_5 peaks were detected, indicating that more Cu_6Sn_5 had formed during reflow. A Cu_3Sn peak was detected at about 50.8° as well.

Cu_6Sn_5 is generally believed to be the first phase to form at the liquid Sn/solid Cu interface when reflow occurs at temperatures below 260°C [12]. During the initial stages of reaction, Cu dissolves rapidly into the molten Sn and forms Cu_6Sn_5 crystallites at the Sn-Cu/Cu interface, according to eq. (1). These crystallites were observed by Gagliano et al. [29] when hot Cu was dipped into molten Sn for 1 s in the temperature range of 240°C to 300°C and the crystallites grew into a continuous layer. The Cu_3Sn layer is located between the Cu substrate and the Cu_6Sn_5 layer. The Cu atoms at the Cu/Cu_6Sn_5 interface react with Cu_6Sn_5 to form Cu_3Sn, according to eq. (2). After a continuous Cu_3Sn layer forms, Cu atoms, represented as [Cu] in eq. (2), continuously diffuse through the formed Cu_3Sn layer and to the Cu_6Sn_5 layer and react with Cu_6Sn_5 to form more Cu_3Sn at the Cu_3Sn/Cu_6Sn_5 interface through the consumption of some of the Cu_6Sn_5. There is likely some Sn diffusion through the interfacial region, but Cu diffusion rates are significantly higher, so Sn diffusion is ignored here.

$$6Cu + 5Sn = Cu_6Sn_5 \quad (1)$$

$$9[Cu] + Cu_6Sn_5 = 5Cu_3Sn \quad (2)$$

In order to study the growth of IMCs at Sn-Cu/Cu interface, reflowed Sn-Cu/Cu samples (260°C, 30 s) were aged at 125°C for 0, 24, 48, and 72 h, and corresponding SEM BSE cross section images are shown in Fig. 3. A continuous bilayer of Cu_3Sn and Cu_6Sn_5 was found in all four samples with a maximum thickness of about 3 μm. The thickness of the Cu_3Sn layer increased as aging time increased, which is due to continuous diffusion of Cu from the Cu substrate to the Cu_3Sn/Cu_6Sn_5 interface and continuous reaction between diffused Cu and Cu_6Sn_5 [eq. (2)].

The Cu_6Sn_5 layer has a morphology that is irregular, which makes it difficult to determine the exact thickness of the

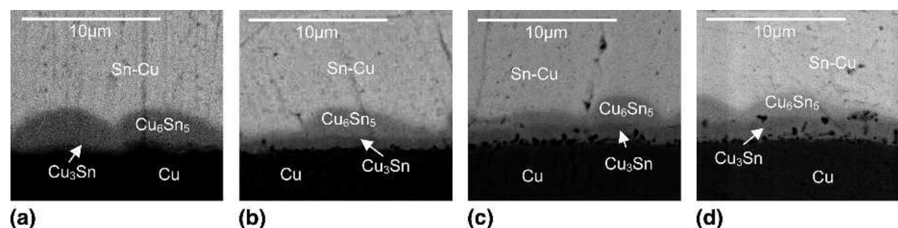

Fig. 3. SEM BSE cross section images of Sn-1.1wt%Cu films electrodeposited onto Cu after reflow and aging. (a) Reflowed at 260°C for 30 s, no aging; (b) reflowed at 260°C for 30 s and aged at 125°C for 24 h; (c) reflowed at 260°C for 30 s and aged at 125°C for 48 h; (d) reflowed at 260°C for 30 s and aged at 125°C for 72 h.

Downloaded from http://meridian.allenpress.com/jmep/article-pdf/7/1/48/2247362/1551-4897-7_1_48.pdf by guest on 01 November 2022

Cu_6Sn_5 layer in each sample. The maximum thickness of the Cu_6Sn_5 layer decreases as aging time is increased, which is due to the consumption of Cu_6Sn_5 to form Cu_3Sn according to eq. (2). It is also possible that some Cu diffuses through to the Cu_6Sn_5/Sn interface to react directly with Sn to form more Cu_6Sn_5:

$$6[Cu] + 5Sn = Cu_6Sn_5 \qquad (3)$$

When the Cu_6Sn_5 consumption rate [eq. (2)] is faster than the Cu_6Sn_5 formation rate [eq. (3)], as is the case here, the thickness of the Cu_6Sn_5 layer will decrease with time.

During the aging process, solid state Sn-Cu/Cu IMC growth is diffusion controlled and can be expressed using the following simple equation [30]:

$$X(t) - X_o \propto (Dt)^{1/2} \qquad (4)$$

where $X(t)$ is the IMC thickness after aging for time t, X_0 is the initial thickness after reflow, and D is the diffusion coefficient, which is related to the growth rate of the Sn-Cu/Cu IMC layer.

The diffusion coefficient D can be calculated when both $X(t)$ and X_0 are known. Unlike the Cu_6Sn_5 layer, the Cu_3Sn layer in each sample is planar. The thickness of the Cu_3Sn layer was determined by averaging measurements taken from at least 10 locations. A plot of Cu_3Sn thickness as a function of the square root of aging time at 125°C is shown in Fig. 4. A diffusion coefficient of 2.3×10^{-14} cm^2/s was determined. The diffusion coefficient was measured by Ma et al. [31] at the same temperature for Sn balls on Cu pads. Their value was more than an order of magnitude higher (6.6×10^{-13} cm^2/s); however, they included the entire IMC layer (both Cu_3Sn and Cu_6Sn_5) in their measurements.

Fine Kirkendall voids were observed not only at the Cu/Cu_3Sn interface, but also inside the Cu_3Sn layer and at the Cu_3Sn/Cu_6Sn_5 interface in aged Sn-1.1Cu/Cu samples, as shown in Fig. 3(b-d). These result from the rapid diffusion of Cu from the Cu layer and through the Cu_3Sn layer. Previous work has shown that both Cu and Sn are mobile within Cu_3Sn, although the diffusion rate of Cu is greater than that of Sn (three times greater at 200°C) [12,21]. Kirkendall voids were also reported to form between electrodeposited Cu and eutectic Pb-Sn after reflow at 220°C and aging at 100-150°C [32], as well as for Ni-doped Sn-Ag [33] and pure Sn [12]. Fig. 3(b-d) shows that as aging time increases, the density of the voids (i.e., the number of voids) at the interface increases. The coalescence of these voids could cause the separation of the Cu_3Sn layer from the Cu substrate, a potential reliability threat.

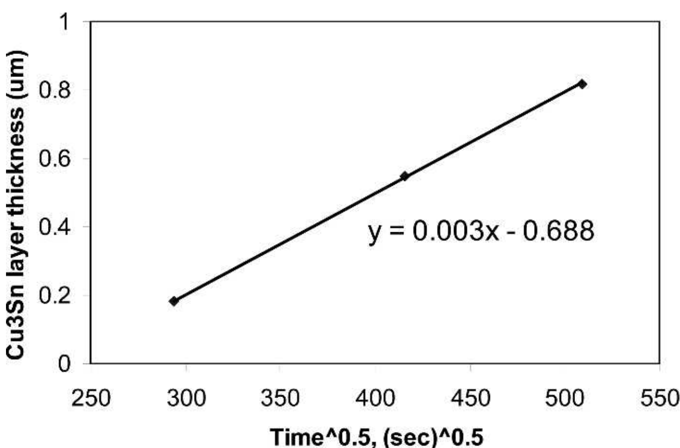

Fig. 4. Plot of Cu_3Sn thickness in Sn-Cu/Cu as a function of square root of aging time at 125°C.

2. Sn-Cu Solder and Ni Substrates

Near eutectic Sn-Cu solder films with the same composition as above were electrodeposited onto Ni to study interfacial reactions between Sn-Cu solders and the Ni substrate during reflow and aging. During reflow at 260°C, molten Sn-Cu spread out quickly and covered the entire sample surface with some differences in thickness at different positions. A low magnification SEM BSE cross section image after reflow is shown in Fig. 5(a). The contact angle between Sn-Cu solder and Ni substrate is low, indicating good wettability between Sn-Cu and Ni. The higher magnification image shown in Fig. 5(b) was taken from an area where the solder thickness was about 3 μm and needle-like grains developed. In order to better reveal the microstructure at the interface, the Sn matrix was selectively etched away and the corresponding SEM BSE image for the sample etched for 5 s is shown in Fig. 5(c). Three different types of morphologies were observed, indicated with arrows in Fig. 5(c): a continuous planar layer at the Ni interface; long, thin needles; and large, polygonal crystals. Similar morphologies were reported by Bader et al. [34] when a system of Sn-Ni was reflowed at 240-400°C. They found that large quantities of Ni_3Sn_4 needles were present after reflowing at 240°C for only 7 s. The first large Ni_3Sn_4 crystals appeared after 30 s and their numbers increased rapidly with continuous reflow. Bader et al. [34] proposed that coarsening of Ni_3Sn_4 needles into large crystals took place. EDX point analysis was performed on all three morphologies of Ni_3Sn_4 in Fig. 5(c) and similar results were obtained: 69-72 wt% Sn (53-56 at%), 22-28 wt% Ni (35-44 at%) and 3-6 wt% Cu (3-9 at%). The compositions correspond to Ni_3Sn_4, or more correctly $(Ni, Cu)_3Sn_4$, which is Ni_3Sn_4 with Cu partially substituting for Ni.

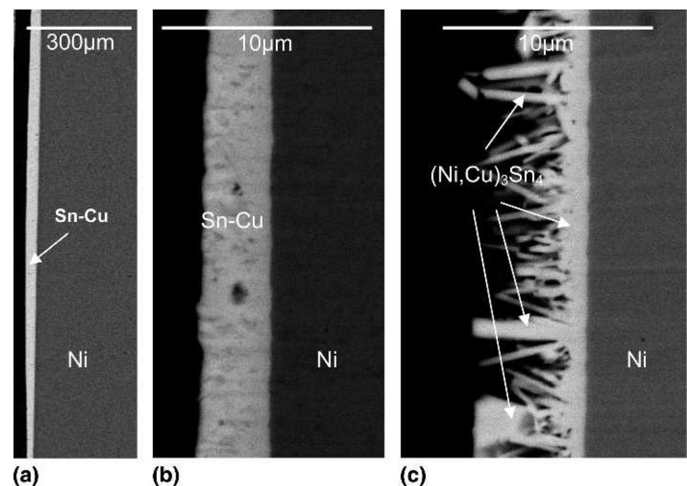

Fig. 5. SEM BSE cross section images of Sn-Cu films electrodeposited onto a substrate of Ni after reflow at 260°C for 90 s. (a) Low magnification image; (b) higher magnification image; (c) higher magnification image after selective etching.

Downloaded from http://meridian.allenpress.com/jmep/article-pdf/7/1/48/2247362/1551-4897-7_1_48.pdf by guest on 01 November 2022

Needles and crystals with similar morphologies were also found at the reflowed Sn-Ag-Cu/Ni interface and were identified as $(Ni,Cu)_3Sn_4$ by TEM analysis (not shown here).

In order to study phase changes in Sn-Cu/Ni before and after reflow, XRD analysis was carried out for as-deposited Sn-Cu/Ni, as-deposited Sn-Cu/Ni after etching, Sn-Cu/Ni after reflow, and Sn-Cu/Ni after reflow and etching [Fig. 6(a-d)]. For as-deposited Sn-Cu/Ni [Fig. 6(a)], two phases were detected, with Sn as the main phase and a small amount of Cu_6Sn_5. After etching away much of the Sn matrix (2% HCl + 5% HNO_3 + 93% CH_3OH), Cu_6Sn_5 peaks at 35.2°, 50.5°, and 62.9° became much more intense, with additional Cu_6Sn_5 peaks detected [Fig. 6(b)]. After reflow at 260°C for 30 s [Fig. 6(c)], the most intense Sn peak changed from Sn (220) to Sn (200). The Cu_6Sn_5 peaks at 21.2° and 43.4° disappeared and additional Cu_6Sn_5 peaks at 41.3° and 94.9° were detected. In order to obtain IMC phase information at the interface, most of the Sn was etched away. The XRD results are shown in Fig. 6(d). Comparing Fig. 6(c) with Fig. 6(d), the Cu_6Sn_5 peaks became much stronger at 35.2° and 50° and four additional Cu_6Sn_5 peaks were detected after etching. This is due to the same reason as explained above for etched Sn-Cu/Cu. In addition, Ni_3Sn_4 was detected, and is referred to here as $(Ni,Cu)_3Sn_4$ because of Cu dissolution in the phase.

The results presented above suggest that during reflow at 260°C, Ni dissolved into the liquid solder until the solder was saturated with Ni. Ni_3Sn_4 nucleation started at the solder/Ni interface and formed a continuous planar layer, from which Ni_3Sn_4 needles grew. With continued reflow, coalescence of Ni_3Sn_4 needles took place, forming large crystals. Meanwhile, Cu at the solder/Ni interface dissolved into Ni_3Sn_4 to form $(Ni,Cu)_3Sn_4$. Nickel diffused into the Sn-Cu solder and dissolved into the existing Cu_6Sn_5 particles to form $(Cu,Ni)_6Sn_5$.

Aging experiments for reflowed Sn-Cu/Ni were carried out and corresponding SEM BSE cross section images are shown in Fig. 7. In all four samples, the regions between the Sn-Cu solder and Ni substrate were characterized by a brighter color which was identified as $(Ni,Cu)_3Sn_4$. As the aging time was increased, the number of $(Ni,Cu)_3Sn_4$ needles decreased and the size of the polygonal $(Ni,Cu)_3Sn_4$ crystals increased, which means that coalescence of $(Ni,Cu)_3Sn_4$ needles into larger $(Ni,Cu)_3Sn_4$ crystals occurred during aging. The thickness of the $(Ni,Cu)_3Sn_4$ layer stayed almost the same after aging for up to 48 h and decreased after aging for 72 h. This may be due to the formation of a linked network structure of $(Ni,Cu)_3Sn_4$.

Comparison of Fig. 3 and Fig. 7 shows that two different types of IMC structures formed for Sn-Cu/Cu and Sn-Cu/Ni after reflow at 260°C for 30 s. In addition, no Kirkendall voids formed at the Sn-Cu/Ni interface even after aging at 125°C for up to 72 h. This may be an indication of similar diffusion rates for Ni, Sn, and Cu.

Downloaded from http://meridian.allenpress.com/jmep/article-pdf/7/1/48/2247362/1551-4897-7_1_48.pdf by guest on 01 November 2022

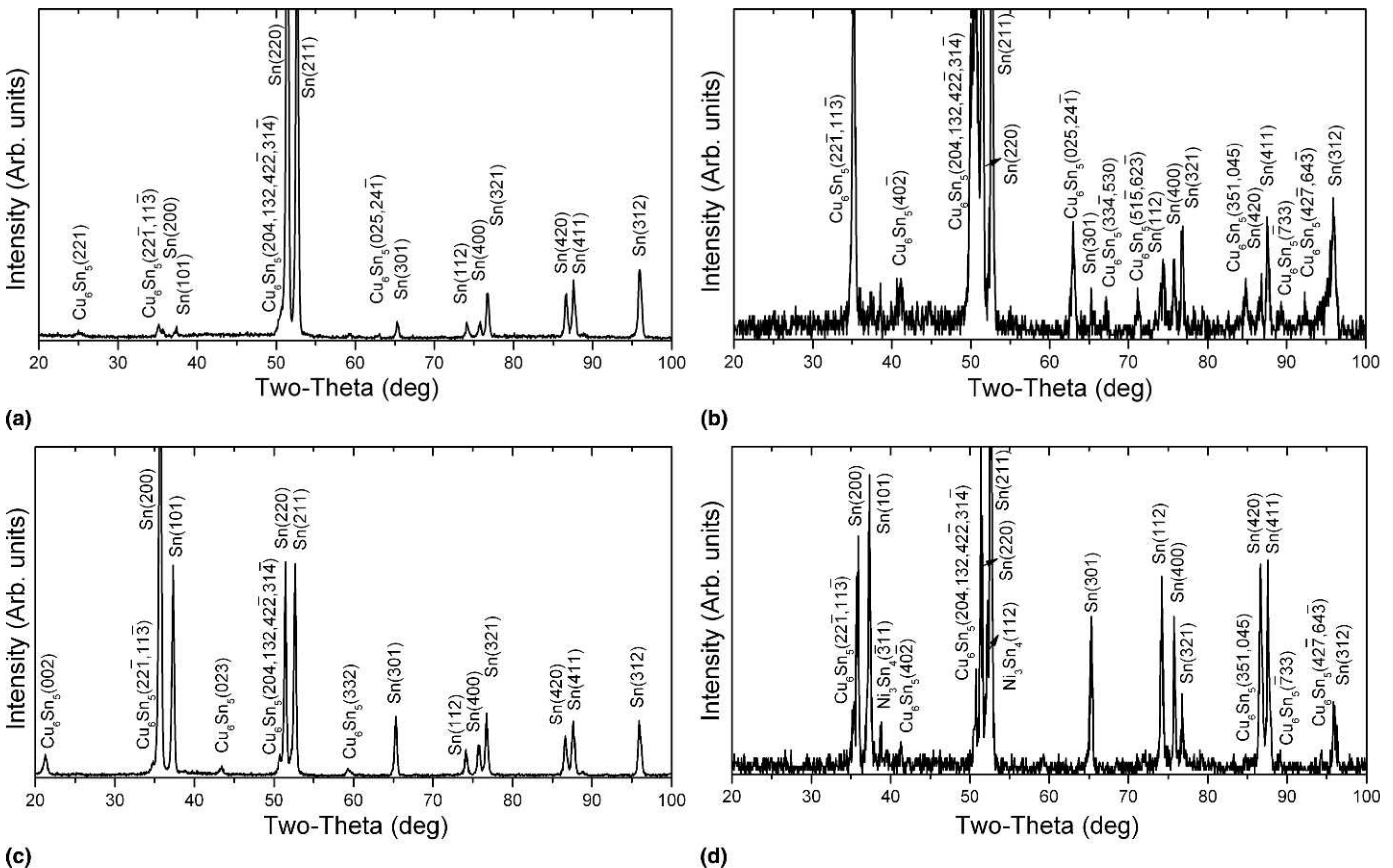

Fig. 6. XRD patterns of Sn-Cu films electrodeposited onto Ni substrate. (a) As-deposited; (b) as-deposited and etched; (c) after reflow at 260°C for 30 s; (d) after reflow at 260°C for 30 s and etched.

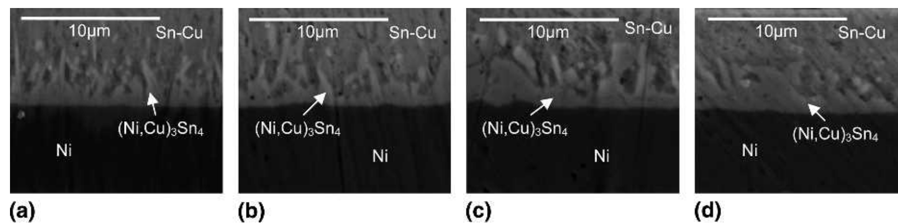

Fig. 7. SEM BSE cross section images of Sn-Cu films electrodeposited onto a substrate of Ni after reflow and aging. (a) Reflowed at 260°C for 30 s; (b) reflowed at 260°C for 30 s and aged at 125°C for 24 h; (c) reflowed at 260°C for 30 s and aged at 125°C for 48 h; (d) reflowed at 260°C for 30 s and aged at 125°C for 72 h.

B. Sn-Ag-Cu Solder

1. Sn-Ag-Cu Solder and Cu Substrates

Sn-3.6Ag-1.8Cu solder films were electrodeposited onto Cu. After etching the as-deposited Sn-Ag-Cu solder films for 5 s, small, bright contrast particles showed up in the SEM BSE plan view images [Fig. 8(a)]. These particles contained high amounts of Ag, as determined from EDX analysis, and were identified as Ag_3Sn within the Sn matrix. The same high Ag content particles were also found in polished Sn-Ag-Cu/Cu cross section samples, even without etching [Fig. 8(b)]. No pure Ag particles were found in the deposits, which is an indication that solid state diffusion of Ag and Sn had occurred at room temperature, forming Ag_3Sn during the time between electrodeposition and SEM characterization. This phenomenon is well documented for noble metal-Sn systems, such as Au-Sn and Ag-Sn; see, for example, Tang et al. [35].

Ag_3Sn particles were evenly distributed within the solder films. After reflow at 260°C for 30 s, elongated Ag_3Sn particles formed [e.g., arrow in Fig. 8(c)]. EDX analysis of a group of small particles in Fig. 8(c) showed the presence of both Ag and Cu as well as Sn. Since only Ag_3Sn and Cu_6Sn_5 were detected by XRD analysis (Fig. 9), it was assumed that the small particles were mixtures of Ag_3Sn and Cu_6Sn_5 particles. The matrix was identified as Sn by EDX analysis. A cross section image for Sn-Ag-Cu/Cu after reflow [Fig. 8(d)] shows a continuous bilayer of Cu_3Sn (thin) and Cu_6Sn_5 (thick) between the Cu substrate and the solder. Within the solder, Ag_3Sn particles (white) were found in some areas and missing in others. The scratch parallel to the Cu substrate is from polishing.

Three phases were detected by XRD analysis for Sn-Ag-Cu/Cu after reflow, as shown in Fig. 9. The main phase is Sn, with small amounts of Cu_6Sn_5 and Ag_3Sn. The reason only small amounts of Cu_6Sn_5 phase were detected and no Cu_3Sn was detected is because after reflow the sample thickness became nonuniform due to wetting reactions between the solder and the Cu substrate. During XRD analysis, the x-ray beam happened to be directed at a thicker region and was not able to penetrate to the Cu_6Sn_5 and Cu_3Sn intermetallic layers at the interface. The same situation happened for the Ni_3Sn_4 IMC phase in Sn-Cu/Ni after reflow [Fig. 6(c and d)].

An SEM BSE cross section image of Sn-Ag-Cu/Cu after reflow and etching is shown in Fig. 10. As with the Sn-Cu/Cu samples, a uniform thin layer of Cu_3Sn formed adjacent to the Cu substrate and Cu_6Sn_5 formed as a layer between Cu_3Sn and the Sn-Ag-Cu solder with an irregular morphology. The difference is that after reflow at 260°C for 30 s, a thinner Cu_3Sn layer formed in Sn-Ag-Cu/Cu than the one that formed in Sn-Cu/Cu. It appears that the addition of Ag into Sn-Cu solders inhibits the formation of Cu_3Sn during reflow.

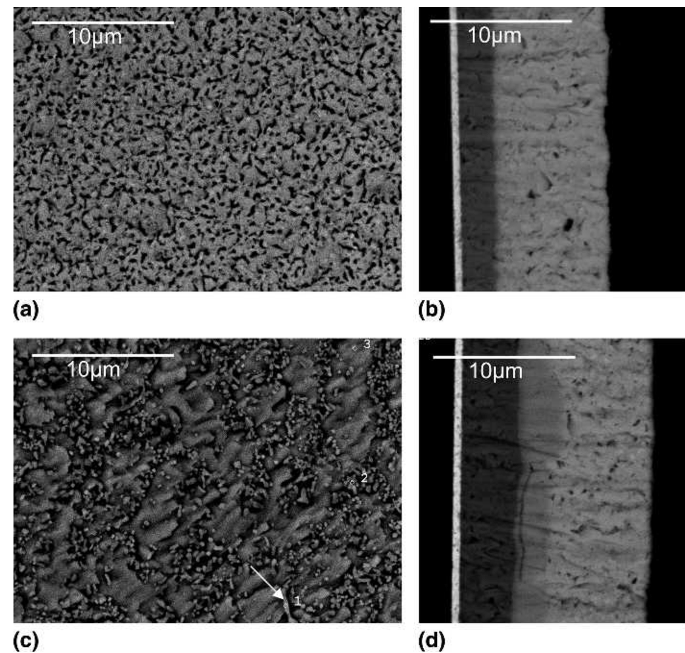

Fig. 8. SEM BSE images of Sn-Ag-Cu film deposited onto a Cu substrate. (a) Plan view, after etching; (b) cross section; (c) plan view, after reflow at 260°C for 30 s and etching; (d) cross section, after reflow at 260°C for 30 s and before etching.

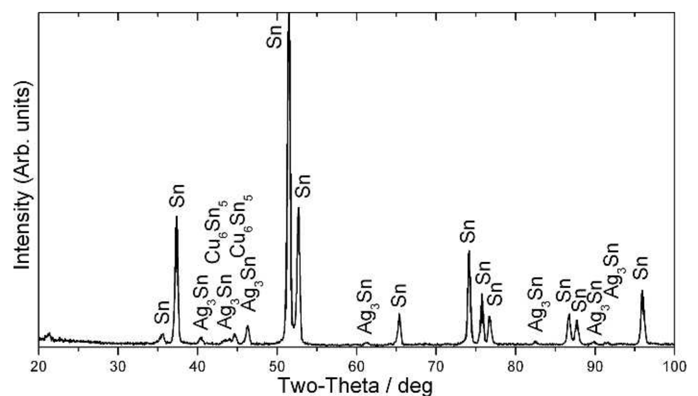

Fig. 9. XRD pattern from Sn-Ag-Cu film after reflow at 260°C for 30 s.

In order to study the aging behavior, Sn-Ag-Cu/Cu samples were reflowed at 260°C for 30 s first and then aged at 125°C for different lengths of time. Corresponding SEM BSE cross

Downloaded from http://meridian.allenpress.com/jmep/article-pdf/7/1/48/2247362/1551-4897-7_1_48.pdf by guest on 01 November 2022

section images are shown in Fig. 11, both without and with etching. Similar to the Sn-Cu/Cu samples, after aging for up to 72 h, the thickness of the entire IMC layer did not change much. The Cu_3Sn layer became thicker as aging time increased, which is due to the continuous diffusion of Cu from the Cu substrate to the Cu_3Sn/Cu_6Sn_5 interface to react with Cu_6Sn_5 to form Cu_3Sn [eq. (2)]. The decrease in Cu_6Sn_5 thickness can be explained in the same way as for Sn-Cu/Cu samples. The thicknesses of the Cu_3Sn layers in samples after aging for 0, 20, 48, and 72 h were determined by averaging measurements taken from at least 10 locations, and a plot of Cu_3Sn layer diffusion distance as a function of the square root of aging time at 125°C is shown in Fig. 12. The diffusion coefficient D was determined as 3.6×10^{-15} cm^2/s, which is almost one order of magnitude smaller than the D value for Sn-Cu/Cu after aging at the same temperature. Therefore, the addition of Ag into Sn-Cu not only inhibited the formation of Cu_3Sn during reflow (formation of a thinner Cu_3Sn IMC), but also slowed down the growth of the Cu_3Sn layer during aging (inhibited Cu outward diffusion), which should improve the long term reliability of the solder joint. Silver had a similar effect in Sn-Zn-Bi-Ag solders [36], where the presence of a small amount of Ag (0.5-1.0 wt%) slowed down the growth rate of IMCs, particularly Cu_5Zn_8. The authors attributed this to Ag dissolving into Cu_5Zn_8 partially substituting for Cu.

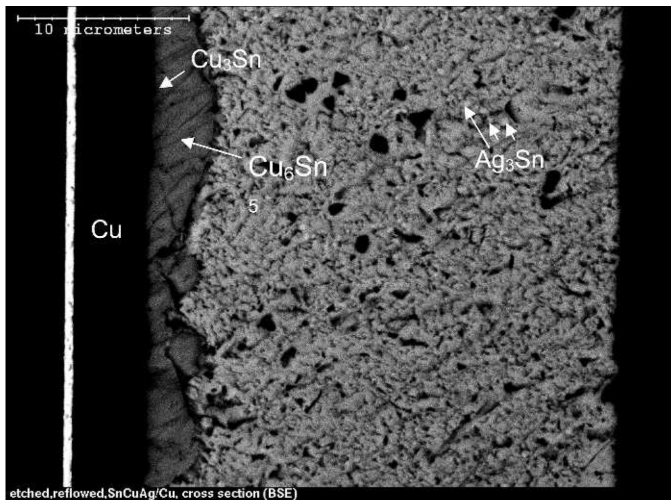

Fig. 10. SEM BSE cross section image of Sn-Ag-Cu film deposited onto Cu substrate after reflow at 260°C for 30 s and etching.

2. Sn-Ag-Cu Solders and Ni Substrates

The same Sn-3.6Ag-1.8Cu solder films as used for the previous section were electrodeposited onto Ni substrates to study the interactions between Sn-Ag-Cu solders and Ni during reflow and aging. SEM SE plan view images of the Sn-Ag-Cu/Ni samples after reflow at 230°C for 30 s and etching for 5 s are shown in Fig. 13. Higher magnification images at locations I and II in Fig. 13(a) are shown in Fig. 13(b and c). Two different types of morphologies were observed: elongated particles and larger round plates. The small circular particles are actually elongated particles in perpendicular or near perpendicular orientations. Similar morphologies were also observed for Sn-Ag-Cu/Ni after reflow at 260°C for 30 s [Fig. 13(d)]. EDX point analysis showed that the elongated particles had high Ag content, similar to the particles in Fig. 8(c), and were identified as Ag_3Sn IMCs within the Sn matrix. Their identity was confirmed by TEM analysis (not shown here) through selected area diffraction (SAD). The elongated particles precipitate from the molten solder.

The round particles were about 200 nm in diameter. EDX point analysis showed that these particles contained Sn, Cu,

Downloaded from http://meridian.allenpress.com/jmep/article-pdf/7/1/48/2247362/1551-4897-7_1_48.pdf by guest on 01 November 2022

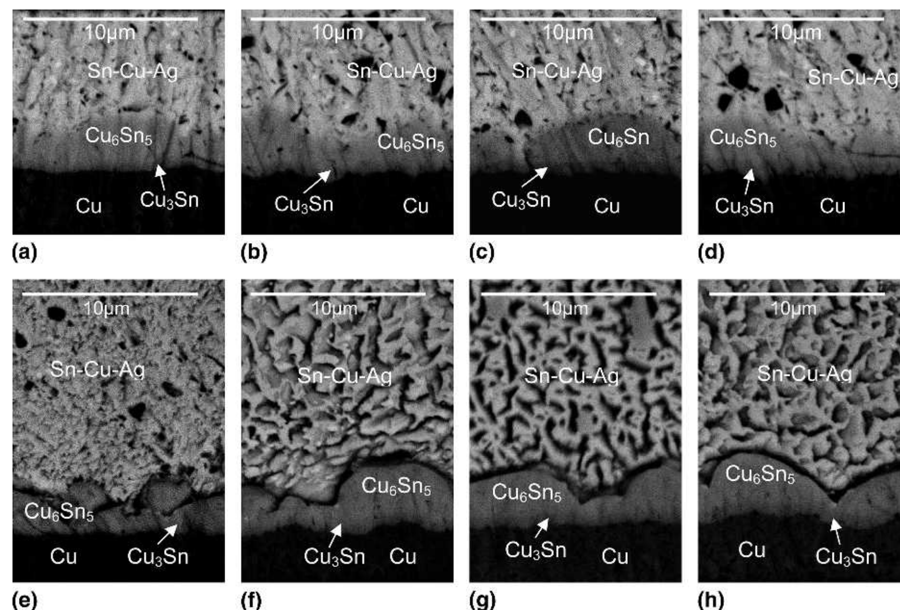

Fig. 11. SEM BSE cross section images of Sn-Ag-Cu films deposited onto Cu substrate after reflow and aging. (a) Reflowed at 260°C for 30 s; (b) reflowed at 260°C for 30 s and aged at 125°C for 24 h; (c) reflowed at 260°C for 30 s and aged at 125°C for 48 h; (d) reflowed at 260°C for 30 s and aged at 125°C for 72 h; (e)-(f) are SEM BSE images of samples (a)-(d) after etching.

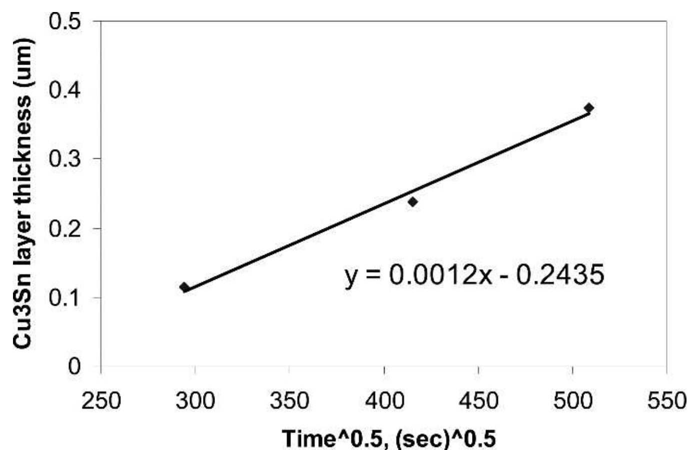

Fig. 12. Plot of Cu_3Sn layer thickness in Sn-Ag-Cu/Cu as a function of the square root of aging time at 125°C.

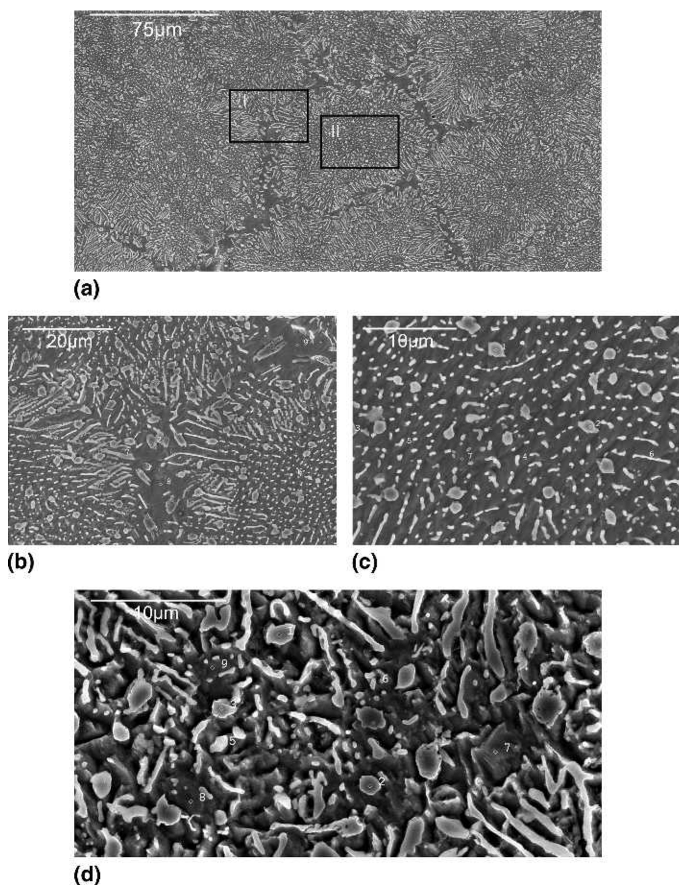

Fig. 13. SEM SE plan view images of Sn-Ag-Cu film deposited onto Ni substrate: (a) after reflow at 230°C for 30 s and etching; (b) higher magnification image at location I in (a); (c) higher magnification image at location II in (a); (d) after reflow at 260°C for 30 s and etching.

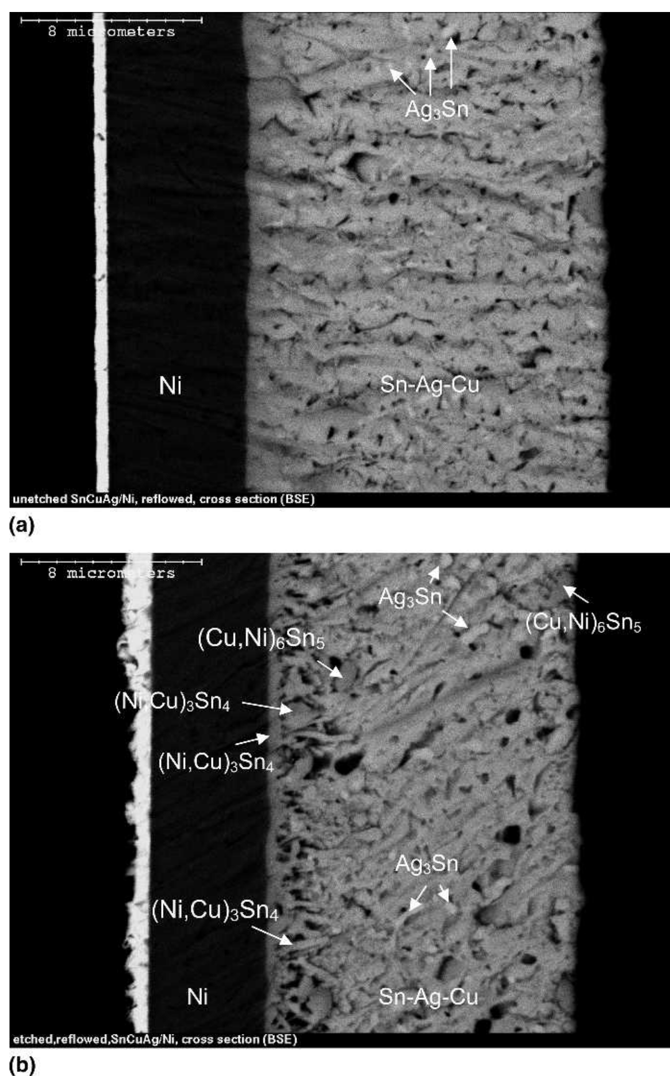

Fig. 14. SEM BSE cross section images of Sn-Ag-Cu film deposited onto Ni substrate. (a) After reflow at 260°C for 30 s, without etching; (b) after etching for 5 s.

and Ni. The Cu content was as high as 23 wt% (32 at%) and the Ni content was as high as 12 wt% (20 at%). The particles were confirmed to be $(Cu,Ni)_6Ni_5$ by SAD analysis in the TEM. When the reflow temperature was increased from 230°C to 260°C, the morphologies of the IMCs looked the same, with an increase in particle densities, as more IMC particles formed at higher temperature.

Fig. 14 shows SEM BSE cross section images of Sn-Ag-Cu/Ni after reflow at 260°C for 30 s without [Fig. 14(a)] and with etching [Fig. 14(b)]. Similar to the reflowed Sn-Ag-Cu/Cu samples, the small bright particles [e.g., arrows in Fig. 14(a)] were identified as Ag_3Sn, and are marked in both Fig. 14(a) and Fig. 14(b). Large Cu_6Sn_5 particles, with significant amounts of Ni dissolution, are also indicated by arrows in Fig. 14(b), and are specified as $(Cu,Ni)_6Sn_5$, since Ni substitutes for Cu.

After etching for 5 s, three different morphologies at the Sn-Ag-Cu/Ni interface were observed [Fig. 14(b)]: a continuous planar layer at the Ni interface, long, thin needles, and large, polygonal crystals, which are similar to the interface structure of the reflowed and etched Sn-Cu/Ni sample shown in Fig. 7(c). EDX analysis at these positions gave a composition of about 60 at%Sn, 30 at%Ni, and 10 at%Cu. The continuous planar layer adjacent to the Ni layer, which corresponds to the same

Downloaded from http://meridian.allenpress.com/jmep/article-pdf/7/1/48/2247362/1551-4897-7_1_48.pdf by guest on 01 November 2022

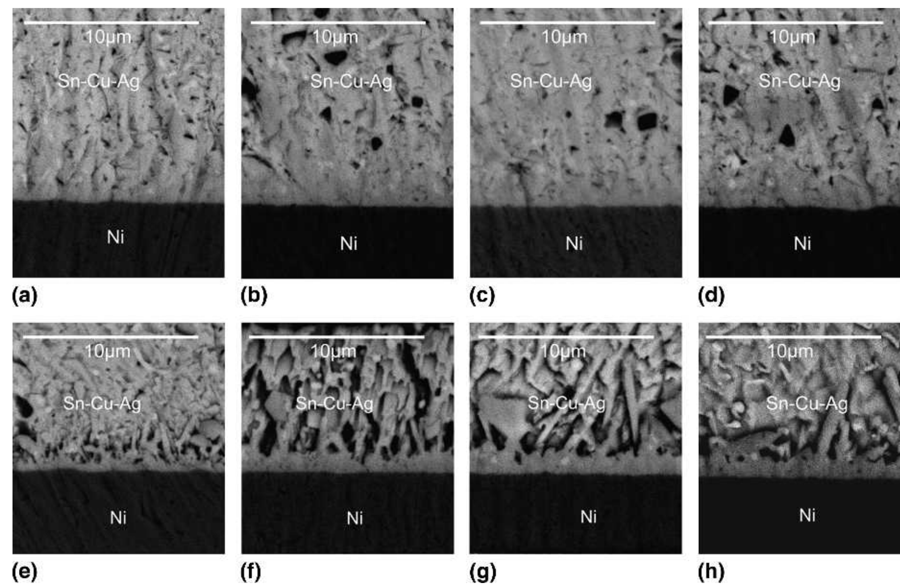

Fig. 15. SEM BSE cross section images of Sn-Ag-Cu films deposited onto Ni substrate after reflow and aging. (a) Reflowed at 260°C for 30 s; (b) reflowed at 260°C for 30 s and aged at 125°C for 24 h; (c) reflowed at 260°C for 30 s and aged at 125°C for 48 h; (d) reflowed at 260°C for 30 s and aged at 125°C for 72 h; (e)-(f) are SEM BSE images of sample (a)-(d) after etching.

location in Fig. 14(a), was identified as $(Ni,Cu)_3Sn_4$. Comparison of Fig. 7(c) and Fig. 14(b) shows that both the continuous planar layer and the layer of needles and crystals are much thinner in reflowed Sn-Ag-Cu/Ni than in reflowed Sn-Cu/Ni, which means the addition of Ag inhibited the formation of $(Ni,Cu)_3Sn_4$ during reflow at 260°C.

After reflow at 260°C for 30 s, Sn-Ag-Cu/Ni samples were aged at 125°C for different lengths of time to study the effect of aging on IMC growth. Fig. 15 shows SEM BSE cross section images of reflowed Sn-Ag-Cu/Ni after aging for 0, 24, 48, and 72 h without etching [Fig. 15(a-d)] and with etching [Fig. 15(e-h)]. As shown in the images without etching, as aging time was increased, the size of the Ag_3Sn particles increased due to Ostwald ripening. To better show the interfacial structures between Sn-Ag-Cu and Ni substrate, all aged samples were etched for 5 s. After aging for 24 h, the continuous planar layer adjacent to the Ni became thicker, while after aging for 48 h and 72 h, the thickness of the continuous planar player did not change much. In addition, the amount of long, thin needles between the continuous planar layer and solder decreased and the size of the polygonal crystals increased. This indicates that during aging, thin needles and polygonal crystals coalesced to form larger needles and crystals.

Conclusions

Interfacial reactions between Sn-1.1Cu and Sn-3.6Ag-1.8Cu solder films and Cu or Ni layers, after reflow and aging, were studied. Since Sn is the main constituent in both solders, the reactions between Sn and the Ni or Cu layers were the main processes during reflow and aging.

When Cu is used as the seed layer, a continuous bilayer of Cu_3Sn (thin, planar) and Cu_6Sn_5 (thick, irregular) formed between the Cu and the solder after reflow at 260°C for both solders. The Cu_3Sn layer at the Sn-Ag-Cu/Cu interface is thinner than that at the Sn-Cu/Cu interface, indicating that the presence of Ag inhibited the formation of Cu_3Sn during reflow. After aging at 125°C, the thickness of the Cu_3Sn layer increased as aging time increased for both Sn-Cu/Cu and Sn-Ag-Cu/Cu. Calculated diffusion coefficients of Cu through the Cu_3Sn layer were 2.25×10^{-14} cm^2/s and 3.6×10^{-15} cm^2/s, respectively. The lower diffusion coefficient for Sn-Ag-Cu/Cu compared with that for Sn-Cu/Cu indicates that the addition of Ag slowed down the growth of the Cu_3Sn layer during aging at 125°C.

When Ni is used as the seed layer, $(Ni,Cu)_3Sn_4$ IMCs with three different morphologies formed at the solder/Ni interface after reflow at 260°C for both Sn-1.1Cu and Sn-3.6Ag-1.8Cu solders: a continuous planar layer adjacent to the Ni, long and thin needles, and large, polygonal crystals. Both the continuous planar layer and the layer of needles and crystals are much thinner in reflowed Sn-Ag-Cu/Ni than in reflowed Sn-Cu/Ni, which means the addition of Ag inhibited the formation of $(Ni,Cu)_3Sn_4$ when reflowed at 260°C. After aging at 125°C for different lengths of time, the continuous planar $(Ni,Cu)_3Sn_4$ layer became thicker, while the entire $(Ni,Cu)_3Sn_4$ IMC layer did not change much for either Sn-1.1Cu or Sn-3.6Ag-1.8Cu solders. The thin needles and polygonal crystals coarsened to form large needles and crystals. Ag_3Sn particles continuously elongated and coarsened during aging and formed longer or larger Ag_3Sn particles. Nickel continuously diffused into the solder layer and dissolved into the $(Cu,Ni)_6Sn_5$ particles. In addition, the $(Cu,Ni)_6Sn_5$ particles coarsened and formed larger and higher Ni content $(Cu,Ni)_6Sn_5$ particles.

Acknowledgments

The authors thank the Natural Sciences and Engineering Research Council (NSERC) of Canada for providing research funding and Micralyne Inc. for providing metalized silicon wafers.

Downloaded from http://meridian.allenpress.com/jmep/article-pdf/7/1/48/2247362/1551-4897-7_1_48.pdf by guest on 01 November 2022

References

[1] J.W. Evans, D. Kwon, and J.Y. Evans, “A Guide to Lead-free Solders: Physical Metallurgy and Reliability,” Springer-Verlag London Limited, London, 2007.

[2] K. Suganuma, “Advances in lead-free electronics soldering,” Current Opinion in Solid State and Materials Science, Vol. 5, pp. 55-64, 2001.

[3] K.J. Puttlitz and K.A. Stalter, “Handbook of Lead-free Solder Technology for Microelectronic Assemblies,” Marcel Dekker, Inc., New York, 2004.

[4] M. Abtew and G. Selvaduray, “Lead-free solders in microelectronics,” Materials Science and Engineering, R: Reports, Vol. 27, pp. 95-141, 2000.

[5] S.K. Kang, P.A. Lauro, D.-Y. Shih, D.W. Henderson, and K.J. Puttlitz, “Microstructure and mechanical properties of lead-free solders and solder joints used in microelectronic applications,” IBM Journal of Research and Development, Vol. 49, pp. 607-620, 2005.

[6] K. Zeng and K.N. Tu, “Six cases of reliability study of Pb-free solder joints in electronic packaging technology,” Materials Science and Engineering, R: Reports, Vol. 38, pp. 55-105, 2002.

[7] K. Suganuma, “Lead-free Soldering in Electronics—Science, Technology, and Environmental Impact,” Marcel Dekker, Inc., New York, 2004.

[8] I.E. Anderson, “Development of Sn-Ag-Cu and Sn-Ag-Cu-X alloys for Pb-free electronic solder applications,” Journal of Materials Science, Materials in Electronics, Vol. 18, pp. 55-76, 2007.

[9] D. Shangguan, “Lead-free Solder: Interconnect Reliability,” ASM International, Materials Park, Ohio, 2005.

[10] K.S. Kim, S.H. Huh, and K. Suganuma, “Effects of intermetallic compounds on properties of Sn-Ag-Cu lead-free soldered joints,” Journal of Alloys and Compounds, Vol. 352, pp. 226-236, 2003.

[11] D.G. Kim, J.W. Kim, and S.B. Jung, “Effect of aging conditions on interfacial reaction and mechanical joint strength between Sn-3.0Ag-0.5Cu solder and Ni-P UBM,” Materials Science and Engineering, B, Vol. 121, pp. 204-210, 2005.

[12] T. Laurila, V. Vuorinen, and J.K. Kivilahti, “Interfacial reactions between lead-free solders and common base materials,” Materials Science and Engineering, R: Reports, Vol. 49, pp. 1-60, 2005.

[13] H. Ipser, H. Flandorfer, C. Luef, C. Schmetterer, and U. Saeed, “Thermodynamics and phase diagrams of lead-free solder materials,” Journal of Materials Science, Materials in Electronics, Vol. 18, pp. 3-17, 2007.

[14] C. Yu, H. Lu, and S. Li, “Effect of Zn addition on the formation and growth of intermetallic compound at Sn-3.5wt%Ag/Cu interface,” Journal of Alloys and Compounds, Vol. 460, pp. 594-598, 2008.

[15] Z. Marinkovic and V. Simic, “Room temperature interactions in Ni/metal thin film couples,” Thin Solid Films, Vol. 98, pp. 95-100, 1982.

[16] S.W. Chen, C.M. Chen, and W.C. Liu, “Electric current effects upon the Sn/Cu and Sn/Ni interfacial reactions,” Journal of Electronic Materials, Vol. 27, pp. 1193-1198, 1998.

[17] S.W. Chen, S.H. Wu, and S.W. Lee, “Interfacial reactions in the Sn-(Cu)/Ni, Sn-(Ni)/Cu, and Sn/(Cu,Ni) system,” Journal of Electronic Materials, Vol. 32, pp. 1188-1194, 2003.

[18] W.T. Chen, C.E. Ho, and C.R. Kao, “Effect of Cu concentration on the interfacial reactions between Ni and Sn-Cu solders,” Journal of Materials Research, Vol. 17, pp. 263-266, 2002.

[19] C.E. Ho, R.Y. Tsai, Y.L. Lin, and C.R. Kao, “Effect of Cu concentration on the reactions between Sn-Ag-Cu solders and Ni,” Journal of Electronic Materials, Vol. 31, pp. 584-590, 2002.

[20] W.C. Luo, C.E. Ho, J.Y. Tsai, Y.L. Lin, and C.R. Kao, “Solid-state reactions between Ni and Sn-Ag-Cu solders with different Cu concentrations,” Materials Science and Engineering, A, Vol. 396, pp. 385-391, 2005.

[21] C.E. Ho, S.C. Yang, and C.R. Kao, “Interfacial reaction issues for lead-free electronic solders,” Journal of Materials Science, Materials in Electronics, Vol. 18, pp. 155-174, 2007.

[22] S.K. Kang, D.Y. Shih, N.Y. Donald, W. Henderson, T. Gosselin, A. Sarkhel, N.Y.C. Goldsmith, K.J. Puttlitz, and W.K. Choi, “Ag_3Sn plate formation in the solidification of near-ternary eutectic Sn-Ag-Cu,” Journal of the Minerals Metals & Materials Society, Vol. 55, pp. 61-65, 2003.

[23] T.Y. Lee, W.J. Choi, K.N. Tu, J.W. Jang, S.M. Kuo, J.K. Lin, D.R. Frear, K. Zeng, and J.K. Kivilahti, “Morphology, kinetics, and thermodynamics of solid-state aging of eutectic SnPb and Pb-free solders (Sn-3.5Ag, Sn-3.8Ag-0.7Cu and Sn-0.7Cu) on Cu,” Journal of Materials Research, Vol. 17, pp. 291-301, 2002.

[24] N. Dariavach, P. Callahan, J. Liang, and R. Fournelle, “Intermetallic growth kinetics for Sn-Ag, Sn-Cu, and Sn-Ag-Cu lead-free solders on Cu, Ni, and Fe-42Ni substrates,” Journal of Electronic Materials, Vol. 35, pp. 1581-1592, 2006.

[25] C. Han, Q. Liu, and D.G. Ivey, “Electrodeposition of Sn-0.7Cu eutectic alloys from chloride-citrate solutions,” Journal of Applied Surface Finishing, Vol. 3, pp. 119-127, 2008.

[26] C. Han, Q. Liu, and D.G. Ivey, “Electrochemical composite deposition of Sn-Ag-Cu alloys,” Materials Science and Engineering, B, Vol. 164, pp. 172-179, 2009.

[27] J.H.L. Pang, L. Xu, X.Q. Shi, W. Zhou, and S.L. Ngoh, “Intermetallic growth studies on Sn-Ag-Cu lead-free solder joints,” Journal of Electronic Materials, Vol. 33, pp. 1219-1226, 2004.

[28] A.R. Fix, G.A. Lopez, I. Brauer, W. Nuchter, and E.J. Mittemeijer, “Microstructural development of Sn-Ag-Cu solder joints,” Journal of Electronic Materials, Vol. 34, pp. 137-142, 2005.

[29] R.A. Gagliano, G. Ghosh, and M.E. Fine, “Nucleation kinetics of Cu_6Sn_5 by reaction of molten tin with a copper substrate,” Journal of Electronic Materials, Vol. 31, pp. 1195-1202, 2002.

[30] K.N. Tu, J.W. Mayer, and L.C. Feldman, “Electronic Thin Film Science for Electrical Engineers and Materials Scientists,” Macmillan, New York, 1992.

[31] X. Ma, F. Wang, Y. Qian, and F. Yoshiba, “Development of Cu-Sn intermetallic compound at Pb-free solder/Cu joint interface,” Materials Letters, Vol. 57, pp. 3361-3365, 2003.

[32] K. Zeng, R. Stierman, T. Chiu, D. Edwards, K. Ano, and K.N. Tu, “Kirkendall void formation in eutectic SnPb solder joints on bare Cu and its effect on joint reliability,” Journal of Applied Physics, Vol. 97, p. 024508, 2005.

[33] Y.W. Wang, Y.W. Lin, and C.R. Kao, “Kirkendall voids formation in the reaction between Ni-doped SnAg lead-free solders and different Cu substrates,” Microelectronics and Reliability, Vol. 49, pp. 248-252, 2009.

[34] S. Bader, W. Gust, and H. Hieber, “Rapid formation of intermetallic compounds interdiffusion in the Cu-Sn and Ni-Sn systems,” Metallurgica et Materialia, Vol. 43, pp. 329-337, 1995.

[35] W. Tang, A. He, Q. Liu, and D.G. Ivey, “Solid state interfacial reactions in electrodeposited Cu/Sn couples,” Transactions of the Nonferrous Metals Society of China, Vol. 19, pp. 930-935, 2009.

[36] L. Liu, W. Zhou, B. Li, and P. Wu, “Interfacial reactions between Sn-8Zn-3Bi-xAg lead-free solders and Cu substrate,” Journal of Alloys and Compounds, Vol. 482, pp. 90-98, 2009.

Downloaded from http://meridian.allenpress.com/jmep/article-pdf/7/1/48/2247362/1551-4897-7_1_48.pdf by guest on 01 November 2022